Few-Mode Erbium-Doped Fiber Amplifier With High Gain and Low Differential Modal Gain for Mode-Division-Multiplexed Systems

Hao Guo, Ting Li, Fengping Yan, Guobin Ren, Wei Wang, Xiangdong Wang, Qi Qin, Guifang Wu, Jiao Gao, Baoyuan Wang, Haoyu Tan, Wenhua Ren, and Ting Feng

***Abstract*—The increasing development of information technology has led to a higher demand for communication capacity. Moreover, the mode division multiplexing (MDM) is considered one of the important technologies to expand the optical fiber transmission capacity, and the few-mode erbium-doped fiber amplifier (FM-EDFA) is a main device applied for optical fiber loss compensation under long-haul communication transmission systems. This article reports the design and characterization of a six-mode erbium-doped fiber amplifier (6M-EDFA) for MDM systems. A center-depressed optical fiber with a trench-assisted structure, is designed and the adjustment of the relevant parameters is applied to reduce the splice loss between the six-mode erbium-doped fiber (6M-EDF) and the transmission fiber. The results show the lowest splice loss is theoretically 0.293 dB. By analyzing the mode field distribution, two erbium ion doping regions are initially identified, the ring region is further layered, and the doping concentration of the three layers is optimized to achieve high gain and low differential modal gain (DMG) using a genetic algorithm (GA). In the case of core forward pumping of the LP_{01} mode at 1480 nm, the simulation results show that the average gain of 25.7 dB and the DMG of 0.277 dB are obtained at 1550 nm considering the mode coupling. Moreover, a 6-mode MDM transmission system is built to fully verify the performance of the designed amplifier to meet the requirements of the MDM communication system.**

***Index Terms*—Differential modal gain, few-mode erbium-doped fiber amplifier, genetic algorithm, mode division multiplexing.**

Manuscript received 21 April 2023; revised 23 June 2023; accepted 3 July 2023. Date of publication 6 July 2023; date of current version 2 November 2023. This work was supported in part by the National Key Research and Development Program of China under Grant 2021YFB2800904, in part by the National Natural Science Foundation of China under Grants 61827818 and 61975049, and in part by China Postdoctoral Science Foundation under Grant 2022M720395. *(Hao Guo and Ting Li contributed equally to this work.) (Corresponding authors: Fengping Yan; Ting Feng.)*

This work did not involve human subjects or animals in its research

Hao Guo, Ting Li, Fengping Yan, Guobin Ren, Xiangdong Wang, Qi Qin, Guifang Wu, Jiao Gao, Baoyuan Wang, Haoyu Tan, and Wenhua Ren are with the School of Electronic and Information Engineering, Beijing Jiaotong University, Beijing 100044, China (e-mail: 22110015@bjtu.edu.cn; 19111024@bjtu.edu.cn; fpyan@bjtu.edu.cn; gbren@bjtu.edu.cn; 21111017@bjtu.edu.cn; qqin0110@163.com; 22110009@bjtu.edu.cn; 21120047@bjtu.edu.cn; 21120017@bjtu.edu.cn; 21120128@bjtu.edu.cn; whren@bjtu.edu.cn).

Wei Wang is with the School of Physical Science and Engineering, Beijing Jiaotong University, Beijing 100044, China (e-mail: 15111006@bjtu.edu.cn).

Ting Feng is with the Photonics Information Innovation Center, Hebei Provincial Center for Optical Sensing Innovations, Hebei University, Baoding 071002, China (e-mail: wlxyft@hbu.edu.cn).

Color versions of one or more figures in this article are available at https://doi.org/10.1109/JLT.2023.3292888.

Digital Object Identifier 10.1109/JLT.2023.3292888

I. Introduction

With the development of optical fiber communication technology, the transmission capacity of the traditional single-mode fiber communication system is approaching the theoretical limit and cannot meet the needs of the growing communication services [1], [2], [3], [4]. Whereas, the mode-division multiplexing (MDM) is able to achieve the purpose of increasing the optical fiber capacity through the mutual superposition of orthogonal multiple spatial modes, each of which can be regarded as an independent channel [5], [6]. Hence, the MDM technology, using few-mode optical fiber transmission lines, is one of the most effective solutions to increase the transmission capacity for long-haul optical fiber communication systems [7], [8], [9]. When an optical fiber is used for long-haul information transmission, several problems inevitably appear, such as optical signal attenuation, dispersion, crosstalk, and nonlinearity [10], [11], [12], [13], [14], [15], which will indeed increase greatly the difficulty of processing the signal at the receiver end. To resolve the optical signal attenuation, a few-mode erbium-doped fiber amplifier (FM-EDFA) is designed, which can compensate the loss in information transmission, and greatly reduce the cost by amplifying multiple mode signals simultaneously; therefore, the design of FM-EDFA has become one of the current research hotspots in optical fiber communication [16], [17], [18], [19].

Currently, the purpose of FM-EDFA design is mainly to achieve high gain and low differential modal gain (DMG) [20], [21], [22]. The research on FM-EDFA mainly focuses on developing the refractive index distribution of the optical fiber, the doping distribution of the erbium-doped fiber (EDF), and the combination of the pumping modes [23], [24], [25], [26]. The refractive index distribution of the different optical fibers corresponds to several mode field distributions, which not only affects the DMG of FM-EDFA, but also influences the splice loss within the transmission fiber. Therefore, the DMG can be reduced by designing a different optical fiber structure while considering the reduction of the splice loss. The optical fiber, with a ring refractive index distribution, can confine the mode fields of the different modes in a high refractive index ring, which can reduce the DMG by reducing the overlap difference between the signal mode fields and the pumping mode fields. Also, the doping distribution of the EDF can be optimized using the genetic algorithm (GA), which originated from computer

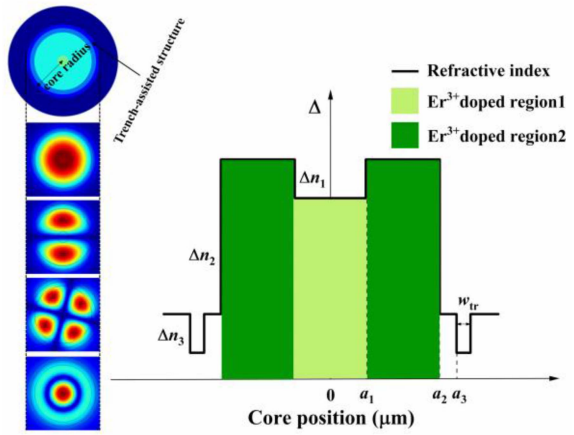

Fig. 1. Mode field distribution and schematic of cross section (left), refractive index and erbium ion concentration profile (right).

simulation studies performed on biological systems. The GA method is a stochastic global search optimization algorithm that plays a very important role in determining the multivariate parameters of the doping range and concentration [27], [28], [29]. In addition, the combination of pumping modes, which achieves the goals of low DMG, is mainly reflected in controlling the mode field intensity distribution of the pumped light.

Based on the abovementioned three ways to reduce DMG, this article analyzes the center-depressed optical fiber with a trench-assisted structure to reduce the splice loss. The doping region and concentration of the six-mode EDF (6M-EDF) is determined by the GA, and the amplification of the optical signal is realized by the LP_{01} forward pumping method. Finally, the feasibility of the designed six-mode EDFA amplifier (6M-EDFA) is validated by building a 6-mode MDM system.

II. Design of 6M-EDFA

Fig. 1 shows the center-depressed 6M-EDF with its trench-assisted structure, is designed to ensure high gain and low DMG characteristics. The fiber core is divided into four layers where the first one is a center depressed structure, the second one is a ring-shaped high refractive index layer, the third one maintains the same refractive index as the cladding layer, and the fourth one is a trench-assisted structure. Moreover, the 6M-EDF supports six linear polarization modes, namely LP_{01}, LP_{11}a, LP_{11}b, LP_{21}a, LP_{21}b, and LP_{02}. The parameters of the optical fiber are set as follow: $\Delta n_1 = 0.598\%$, $\Delta n_2 = 0.797\%$, $\Delta n_3 = -0.2\%$, $a_2 = 7.8\ \mu$m, $a_3 = 9\ \mu$m, and $w_{\rm tr} = 1\ \mu$m. The splice loss between the transmission fiber and EDF, due to the mismatch of the mode field, is an important factor affecting the communication transmission [30], [31], [32]. The transmission fiber is designed a grade-index fiber with a trench-assisted structure. The core radius of the transmission fiber is 11.5 μm, the trench width is 0.7 μm, and the profile exponent is 2.01. By adjusting the a_1 parameter, the splice loss of each mode between the 6M-EDF and the transmission fiber can be obtained as shown in Fig. 2 where one can see that the one of LP_{11} and LP_{21} modes is almost constant when a_1 varies from 0.5 μm to 3 μm, and the splice loss is mainly determined by LP_{01} and LP_{02} modes. The inset shows the total splice loss, which reaches a theoretical minimum at $a_1 = 1.5\ \mu$m. Therefore, the characteristics of the designed 6M-EDF at $a_1 = 1.5\ \mu$m is considered. Observing the mode field distribution in Fig. 1, the uniform doping of the erbium ion in two ranges, namely region1 and region2, is also proposed.

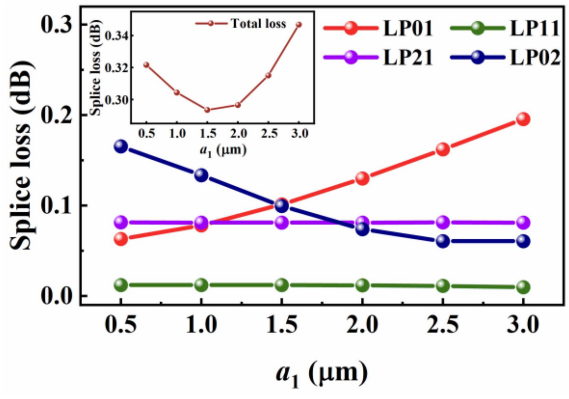

Fig. 2. Splice loss between 6M-EDF and transmission fiber as a function of $a1$.

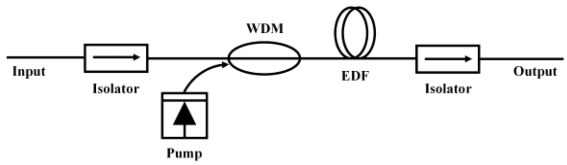

Fig. 3. Simulation structure diagram of 6M-EDFA.

TABLE I
Summary of the Parameters Used in the Simulations

Symbol	Parameter	Value
L	Optical fiber length	10 m
τ	Lifetime of the Er^{3+} upper level	10 ms
P_P	Injected pump power	400 mw
P_S	Signal input power	-10 dBm
λ_P	pump wavelength	1480 nm
λ_S	Signal wavelength	1550 nm
$\sigma_{abs,p}$	Absorption cross-section for the pump	Fig. 4
$\sigma_{abs,s}$ $\sigma_{ems,p}$ $\sigma_{abs,ASE}$ $\sigma_{ems,ASE}$	Absorption and emission cross-section for the signal and ASE	Fig. 4
BW_{ASE}	Noise bandwidth	10 nm

To obtain the gain characteristics of 6M-EDFA, the simulation system is built, as shown in Fig. 3, based on the rate equation and the propagation equation [33], [34]. The input optical signal, through the isolator, is coupled to the EDF with the pump light. The signal light is then amplified by using 1480 nm forward pumping and the initial parameters are shown in Table I. The cross-section absorption and emission indicate the probability that erbium ions will be absorbed and emitted at different wavelengths. Moreover, Fig. 4 shows the absorption and emission spectra of an erbium ion-doped silica fiber used in the simulation. However, the designed 6M-EDFA, using the double layer of uniformly doped 6M-EDF, does not achieve the expected DMG

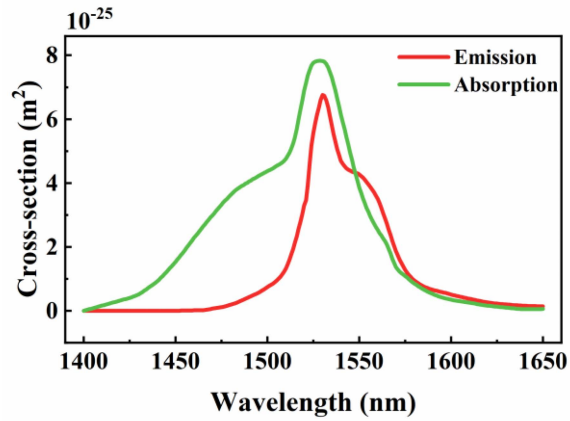

Fig. 4. Absorption and emission cross-sections of the Er^{3+}-doped silica fiber used in simulations.

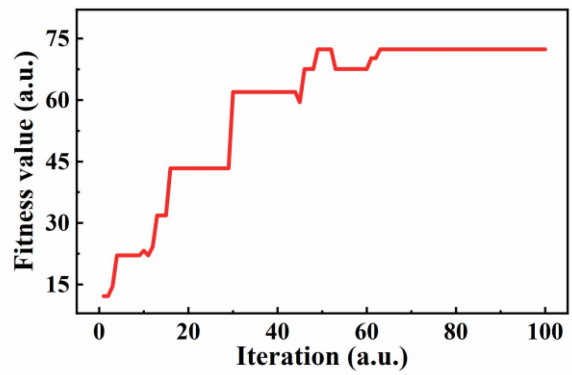

Fig. 5. Change in fitness value for 100 iterations using the GA.

values due to the presence of multiple modes. Based on this situation, region2 is considered for further stratification.

In addition, the three-layer doping method is difficult to yield the most suitable doping structure to meet the demand of low DMG, by manual adjustment, due to the need to calibrate multiple parameters of the doping regions and concentration. Therefore, the GA is introduced to determine these doping variables. In more detail, the GA is coded in binary, the population size is set to 50, and the selection is performed using the roulette wheel method with a crossover and a mutation probabilities of 0.9 and 0.05, respectively. The fitness function F, which determines the fitness of an individual referring to its characteristics, is defined as follows:

$$F = \bar{G}/\Delta G, \tag{1}$$

where $\bar{G}$ represents the average value of gain for each mode and ΔG indicates the maximum value of DMG. The fitness function fully considers the mode average gain and DMG, showing that the doped structures, with large mode average gain and low DMG, are better preserved. Thus, the optimal 6M-EDF can be generated. The fiber doping structure is optimized by using the process of individual coding, the initialization of the population, the calculation of individual fitness, the selection crossover mutation, and the population evolution. The change in the fitness value is obtained after 100 iterations as shown in Fig. 5. The most suitable individual is selected from 100 iterations, and the optimal doping structure is obtained by closely tuning the region range and the concentration values. The optimal doping structure is defined as follows:

$$N_0(r,\varphi) = \begin{cases} 9.5\times10^{24}, & 0\,\mu\text{m} < r \le 1.5\,\mu\text{m} \\ 5.5\times10^{24}, & 1.5\,\mu\text{m} < r \le 6.62\,\mu\text{m} \\ 2.3\times10^{25}, & 6.62\,\mu\text{m} < r \le 7.8\,\mu\text{m} \end{cases}, \tag{2}$$

where N_0 indicates the doping concentration and r represents the radial erbium ion doping radius of the optical fiber. The 6M-EDFA, with this doping structure, features better gain characteristics.

For the actual fabrication of EDF, fiber preform is prepared in a conventional modified chemical vapor deposition (MCVD) process. The high-purity material is first deposited on the inner surface of a quartz glass tube in the structure of the fiber preform. One end of the quartz glass tube is connected to a chemical feed system so that the various chemical materials are mixed in controlled amounts and fed into the quartz glass tube. The composition of the chemical mixture for the corresponding deposited layer is changed according to the process design to obtain the necessary core and cladding optical waveguide structure. During the deposition of the core layer, we injected the corresponding concentration of Er ions solution in layers for soaking. After drying the deposited quartz glass tube is fused and shrunk into a solid quartz glass prefabricated rod. The prepared EDF preforms are calculated, cased with a quartz tube of the appropriate geometry and then drawn to make them.

The refractive index difference between the designed core area and the cladding layer is less than 1% and the refractive index difference between the trench and the cladding layer is greater than -0.5%, and the designed concentration of Er-doped ions can be fully achieved with the existing process. Considering the limitations of the actual active fiber fabrication process and reducing the error between the simulation results and the fabricated object. In the design process, it is ensured that the doped Er ions do not cross the refractive index distribution, which greatly reduces the process difficulty and cost.

III. Gain Characteristics of 6M-EDFA

Using the GA-optimized EDF structure for the 6-mode amplification, the modal gain and the DMG, being considered as a function of optical fiber length, are obtained at the 6M-EDF length of 10 m as shown in Fig. 6(a). As the optical fiber length varies from 0 m to 10 m, the pump light is fully used and the gain of each mode reaches the saturation level. Moreover, the 6M-EDFA achieves a gain of more than 25 dB per mode and a maximum DMG of 0.280 dB, which reflects the good amplification characteristics of 6M-EDFA. As for the noise factor (NF), it is a crucial parameter to measure the amount of noise affecting the signal when applying the fiber amplifier gain [35], [36]. Fig. 6(b) shows the variation of the forward and backward amplified spontaneous emission (ASE) power, and the maximum NF obtained for a 10 m-long 6M-EDF is 3.78 dB. In practical applications, optical fibers are certainly subject to various disturbances. These disturbances include both

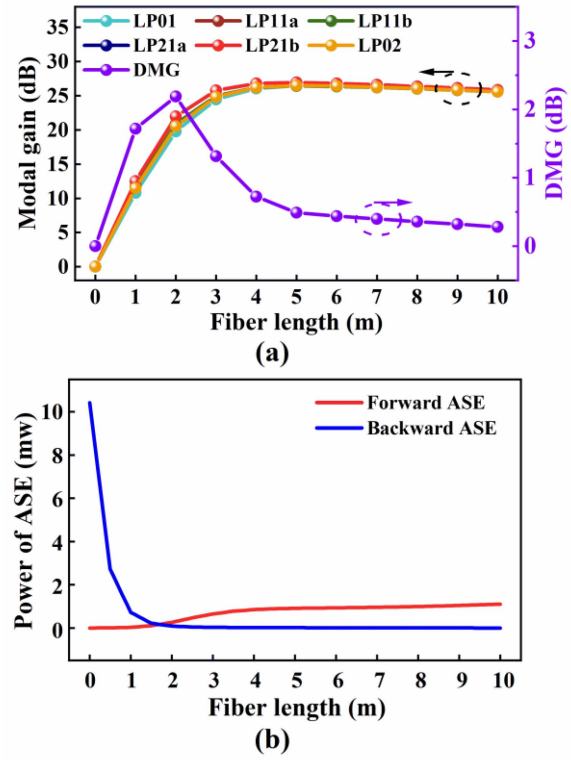

Fig. 6. Simulation results for (a) gain characteristics and (b) ASE power of 10 m 6M-EDF at the parameters in Table I.

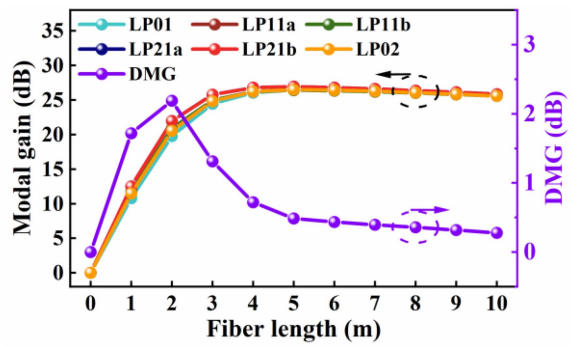

Fig. 7. Variations of the modal gain and DMG with the 6M-EDF length at the parameters in Table I.

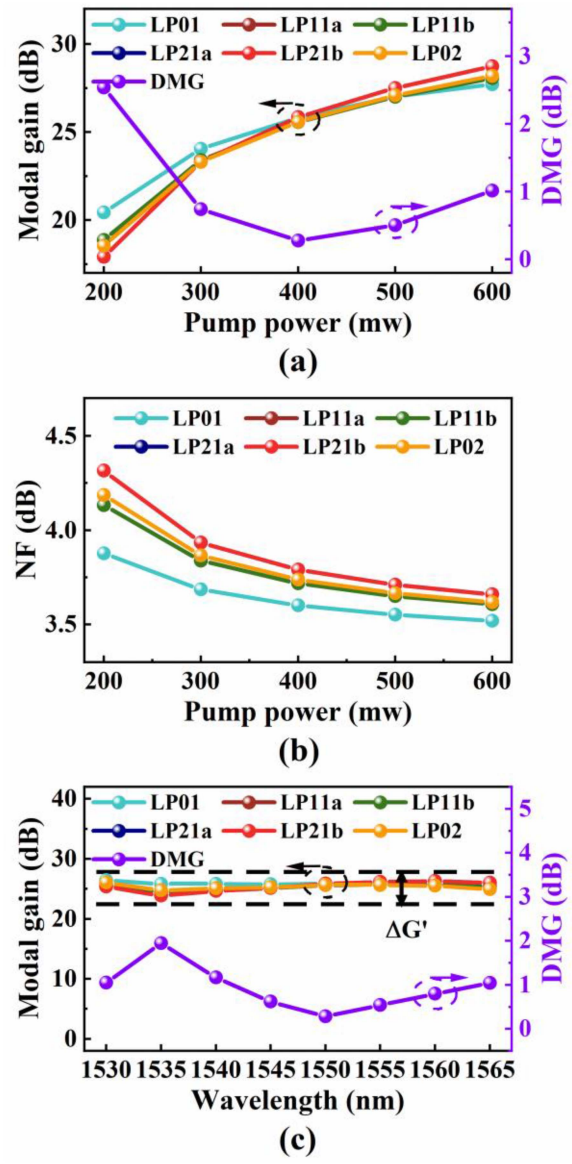

Fig. 8. (a) The amplification characteristics of the 6M-EDFA with different pumping powers at 10 m 6M-EDF. (b) The NF of the 6M-EDFA with different pumping powers at 10 m 6M-EDF. (c) The amplification characteristics of the 6M-EDFA at C-band.

external factors (such as bending, twisting, and stress), and internal factors (caused by imperfect fiber manufacturing processes). Multiple modes will eventually cause mode coupling during transmission if the orthogonality between the modes is compromised [37], [38]. Considering the resulting crosstalk, the gain performance of 6M-EDFA is obtained through modeling the coupled power equation as shown in Fig. 7. Comparing Figs. 6(a) and 7, the mode coupling has little effect on the gain characteristics due to the short design optical fiber length, and the DMG is reduced to 0.277 dB considering the mode coupling.

As for the pump light, it provides the energy for light amplification, allowing lower energy particles to jump to higher energy levels, thereby producing population inversion [39], [40]. Considering the effect of the pump power on the amplification characteristics of the 6M-EDFA, Fig. 8(a) shows the modal gain as a function of pump power for the 6M-EDF at a 10 m length. The modal gain of each mode increases with the pumping power. The $LP_{21}a$ and $LP_{21}b$ modes show the most significant changes, and the LP_{01} mode presents the lowest increase. However, the growth rate of the modal gain gradually slows down with the gradual increase of the pump power. The variation of NF is thereby presented in Fig. 8(b), which becomes lower while the pump power increases, indicating that the higher pump power can improve the performance of the amplifier to some extent; however, considering the nonlinearity caused by high power and the DMG variation, the choice of pump power also needs to be reasonably regulated. Moreover, Fig. 8(c) shows the variation of the modal gain and the DMG with a 5 nm wavelength span in C-band. In addition, the average gain variation of each mode at the considered wavelengths of the signal light in C-band is small,

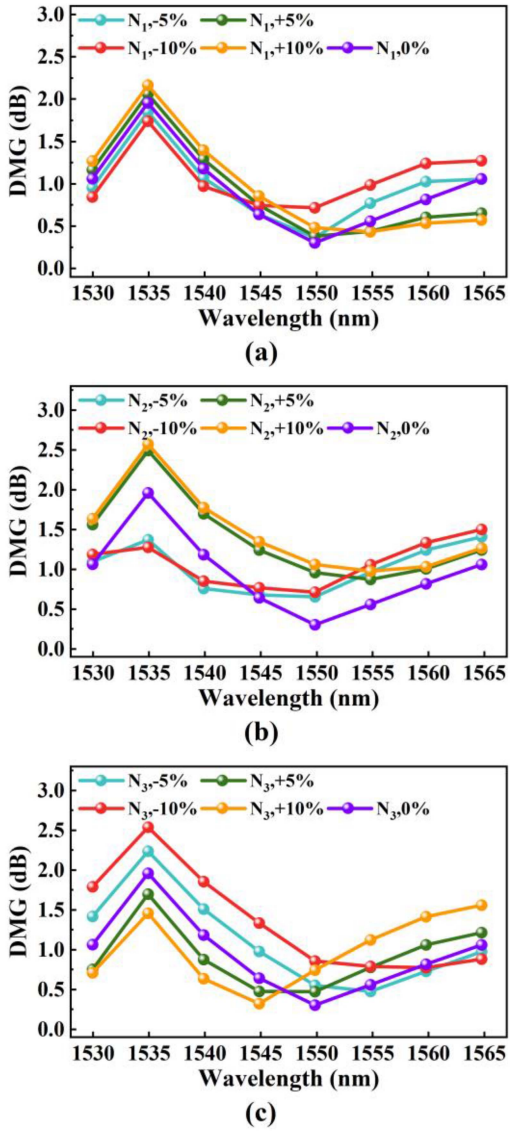

Fig. 9. (a) The effect of N_1 concentration error of the designed EDF on the C-band gain spectrum of the FM-EDFA. (b) The effect of N_2 concentration error of the designed EDF on the C-band gain spectrum of the FM-EDFA. (c) The effect of N_3 concentration error of the designed EDF on the C-band gain spectrum of the FM-EDFA.

and the difference ΔG' between the maximum and minimum values of all modes in the whole C-band is 2.562 dB. The DMG reaches a maximum value of 1.945 dB at 1535 nm, and then gradually decreases before reaching a minimum at 1550 nm. However, the DMG gradually increases again as the signal light wavelength increases from 1550 nm to 1565 nm. In general, the gain and DMG are maintained in a small range and the 6M-EDFA has good gain stability.

The effect of the concentration error of the designed EDF on the C-band gain spectrum of the FM-EDFA is shown in Fig. 9. The errors for the EDF doped structures are set to -5%, $+5\%$, -10%, and $+10\%$ respectively. Fig. 9(a), (b), and (c) corresponds to the effect on the DMG of variations in the doping concentration of the three layers as $N_1 = 9.5 \times 10^{24}$, $N_2 = 9.5 \times 10^{24}$, and $N_3 = 9.5 \times 10^{24}$. Overall, the concentration

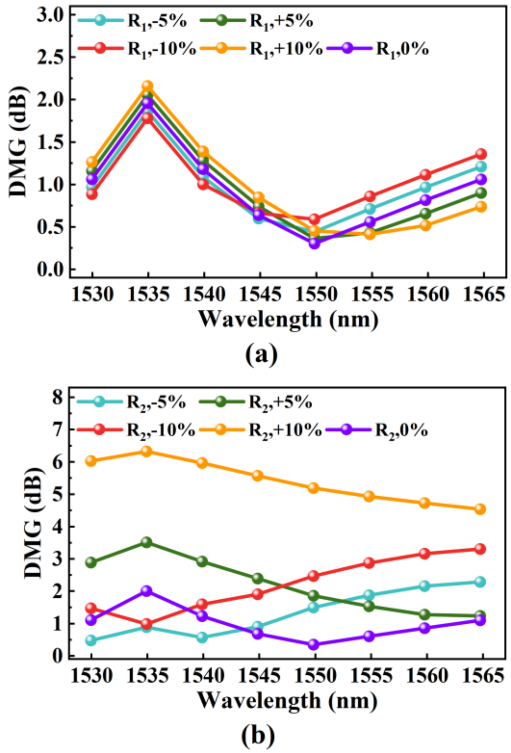

Fig. 10. (a) The effect of R_1 radius error of the designed EDF on the C-band gain spectrum of the FM-EDFA. (b) The effect of R_2 radius error of the designed EDF on the C-band gain spectrum of the FM-EDFA.

error has a smaller effect on the DMG, and the error in N_2 and N_3 have a larger effect on the DMG than N_1. The effect of the concentration errors on DMG value varies by less than 1 dB for the whole C-band, indicating the stability of the designed EDF structure. Fig. 10 shows the effect of varying the doping thickness on the DMG. $R_1 = 1.5$ μm and $R_2 = 6.62$ μm are the radius between the optimized doping layers respectively. The error in R_1 has a small effect on the gain characteristics of the FM-EDFA, while the R_2 has a more pronounced effect on the DMG. The effect of the error on the DMG value is less than 2 dB for the whole C-band when the R_2 is reduced, and the effect on the DMG is small. As R_2 increases, the second layer of the doped structure becomes thicker, the third layer becomes narrower, and the DMG increases as R_2 increases. The maximum DMG value reaches more than 6 dB for a 10% increase in R_2. Therefore, the actual fabrication of the designed EDF should take care to dope the inner layer as much as possible, which provides a reference for the actual fabrication of the fiber.

IV. MDM Transmission Based on the 6M-EDFA

To verify the feasibility of 6M-EDFA in the MDM system, this latter is built as shown in Fig. 11. Considering that the polarization division multiplexing (PDM) can improve the transmission capacity, a 1550 nm laser is used at the transmitter end to generate two polarized beams through the polarization beam splitter (PBS). Afterward, both systems are separately modulated by the IQ (in-phase and quadrature) and transmitted to the transmission fiber through a mode multiplexer under

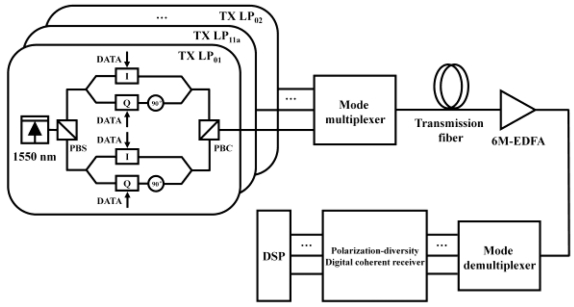

Fig. 11. Simulation structure diagram of PDM-MDM transmission.

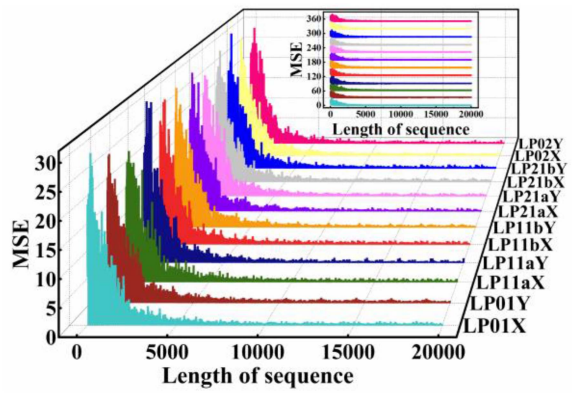

Fig. 12. Convergence under CMA equalization algorithm.

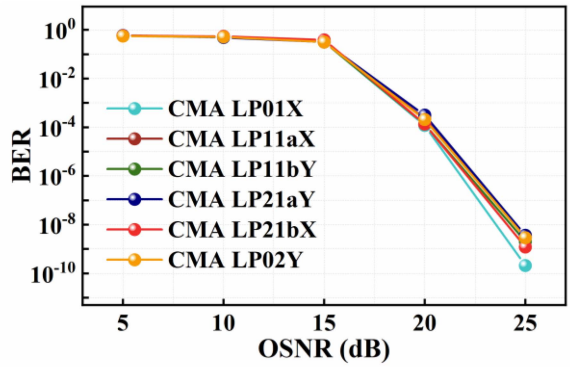

Fig. 13. Comparison of BER at different OSNR for modes $LP_{01}X$, $LP_{11}aX$, $LP_{11}bY$, $LP_{21}aY$, $LP_{21}bX$, and $LP_{02}Y$.

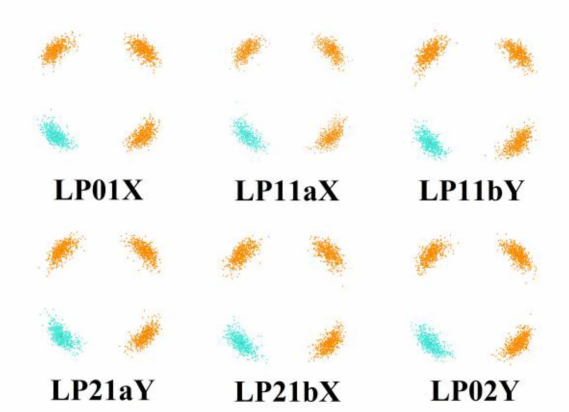

Fig. 14. Constellation diagram after CMA equalization and phase adjustment at 20 dB for modes $LP_{01}X$, $LP_{11}aX$, $LP_{11}bY$, $LP_{21}aY$, $LP_{21}bX$, and $LP_{02}Y$.

the polarization beam combiner (PBC). A polarization-diversity digital coherent receiver subsequently gets the demultiplexed six mode signals after the developed 6M-EDFA has amplified the optical signal. Then, this receiver converts the optical signal into a digital signal and generates the signal after resampling, dispersion compensation, equalization, and carrier recovery through digital signal processing.

The simulation uses the 60 km transmission fiber, and the laser at the transmitter end is modulated at 10 Gbit/s 4-quadrature amplitude modulation (4-QAM) signal, which is equalized using the constant modulus algorithm (CMA) after the dispersion compensation. The convergence of the CMA is obtained with a filter number of taps of 79 and an iteration step of $1e^{-4}$ is shown in Fig. 12. The mean square error (MSE) of each mode decreases continuously with the increase of the sequence length and finally remains at a very low value. Furthermore, the bit error ratio (BER) is an important index reflecting the quality of communication. The simulation set a sequence length of 2048 per block. The BER, as a function of optical signal noise ratio (OSNR) after 100 iterations, is presented in Fig. 13. The BER value decreases gradually as the OSNR increases, and the maximum BER is 3.2×10^{-4} at the OSNR of 20 dB. Fig. 14 shows the constellation diagram of each mode with $LP_{01}X$, $LP_{11}aX$, $LP_{11}bY$, $LP_{21}aY$, $LP_{21}bX$, and $LP_{02}Y$ after the carrier recovery, which features obvious boundaries and compactness. These results verify the reliability of the communication system and that the designed 6M-EDFA can greatly meet the requirements of the MDM communication.

V. Conclusion

We designed the 6M-EDF through simulation and investigated the gain characteristics of the 6M-EDFA system. The splice loss between the 6M-EDF and the transmission fiber is reduced by designing the center-depressed optical fiber with the trench-assisted structure. The signal light is amplified through forward pumping at 1480 nm, and the GA is used to determine the doping structure of the optical fiber to achieve a higher gain and lower DMG of 0.280 dB. The coupled power equation is introduced to reflect the amplification characteristics of the 6M-EDFA under the mode coupling. Due to the short length of the 6M-EDFA, the mode coupling has less effect on the gain characteristics, and the DMG is reduced to 0.277 dB. The 6M-EDFA also shows a good amplification effect in the whole C-band. The difference $\Delta G'$ between the maximum and minimum values of all modes in the whole C-band is 2.562 dB. However, the above conclusions are based on the theoretical calculation, and the actual FM-EDFA is subject to the influence of the fiber processing process, fiber loss, random crosstalk, and the environment, resulting in some deviations in the obtained DMG and an inability to guarantee the 3rd digit accuracy. Therefore, the theoretically obtained DMG is considered to be 0.3 dB with a standard deviation of 0.1 or 0.2 dB.

In addition, considering the effect of the designed 6M-EDFA in the MDM transmission system, the PDM-MDM transmission

system was also built. After the system equalization using the CMA, the BER of each mode is less than 10^{-3} at an OSNR of 20 dB, and the constellation diagram of the modes can be well distinguished, which fully demonstrates the reliability of the transmission system.

REFERENCES

[1] M. Ohashi, K. Shiraki, and K. Tajima, "Optical loss property of silica-based single-mode fibers," *J. Lightw. Technol.*, vol. 10, no. 5, pp. 539–543, May 1992.

[2] E. Agrell et al., "Roadmap of optical communications," *J. Opt.*, vol. 18, no. 6, 2016, Art. no. 063002.

[3] D. Marcuse and C. Lin, "Low dispersion single-mode fiber transmission-the question of practical versus theoretical maximum transmission bandwidth," *IEEE J. Quantum Electron.*, vol. 17, no. 6, pp. 869–878, Jun. 1981.

[4] A. D. Ellis, J. Zhao, and D. Cotter, "Approaching the non-linear Shannon limit," *J. Lightw. Technol.*, vol. 28, no. 4, pp. 423–433, Feb. 2010.

[5] Z. Wan et al., "Divergence-degenerate spatial multiplexing towards future ultrahigh capacity, low error-rate optical communications," *Light Sci. Appl.*, vol. 11, no. 1, 2022, Art. no. 144.

[6] M. Singh and J. Malhotra, "Performance comparison of 2× 20 Gbit/s-40 GHz OFDM based RoFSO transmission link incorporating MDM of Hermite Gaussian modes using different modulation schemes," *Wireless Pers. Commun.*, vol. 110, pp. 699–711, 2020.

[7] P. Sillard et al., "Few-mode fiber technology, deployments, and systems," *Proc. IEEE*, vol. 110, no. 11, pp. 1804–1820, Nov. 2022.

[8] W. Zhang et al., "Mode division multiplexing communication using microwave orbital angular momentum: An experimental study," *IEEE Trans. Wireless Commun.*, vol. 16, no. 2, pp. 1308–1318, Feb. 2017.

[9] B. J. Puttnam et al., "Space-division multiplexing for optical fiber communications," *Optica*, vol. 8, no. 9, pp. 1186–1203, 2021.

[10] S. Girard et al., "Overview of radiation induced point defects in silica-based optical fibers," *Rev. Phys.*, vol. 4, 2019, Art. no. 100032.

[11] P. K. Dubey and V. Shukla, "Dispersion in optical fiber communication," *Int. J. Sci. Res.*, vol. 3, no. 10, pp. 236–239, 2014.

[12] I. Amiri et al., "Mathematical model analysis of dispersion and loss in photonic crystal fibers," *J. Opt. Commun.*, vol. 44, no. 1, pp. 139–144, 2023.

[13] K.-P. Ho et al., "Mode coupling and its impact on spatially multiplexed systems," *Opt. Fiber Telecommun. VI*, vol. 17, pp. 1386–1392, 2013.

[14] C. Antonelli et al., "Role of polarization-mode coupling in the crosstalk between cores of weakly-coupled multi-core fibers," *Opt. Exp.*, vol. 28, no. 9, pp. 12847–12861, 2020.

[15] D. Lu et al., "Structures of exact and solitary optical solutions for the higher-order nonlinear Schrödinger equation and its applications in mono-mode optical fibers," *Modern Phys. Lett. B*, vol. 33, no. 23, 2019, Art. no. 1950279.

[16] Y. Jung et al., "Cladding pumped few-mode EDFA for mode division multiplexed transmission," *Opt. Exp.*, vol. 22, no. 23, pp. 29008–29013, 2014.

[17] Y. Chang et al., "Demonstration of an all-fiber cladding-pumped FM-EDFA with low differential modal gain," *Opt. Laser Technol.*, vol. 155, 2022, Art. no. 108446.

[18] J. Zhu et al., "Weakly-coupled MDM-WDM amplification and transmission based on compact FM-EDFA," *J. Lightw. Technol.*, vol. 38, no. 18, pp. 5163–5169, Sep. 2020.

[19] W. Xu et al., "Gain characteristics of few-mode EDFA with different pump," *IEEE Photon. J.*, vol. 14, no. 5, Oct. 2022, Art. no. 7148607.

[20] J. Ma et al., "Amplification of 18 OAM modes in a ring-core erbium-doped fiber with low differential modal gain," *Opt. Exp.*, vol. 27, no. 26, pp. 38087–38097, 2019.

[21] Q. Qiu et al., "Powerful trade-off between DMG and gain characteristics in the l-band high-numerical aperture few-mode erbium-doped fiber amplifier," *Opt. Laser Technol.*, vol. 158, 2023, Art. no. 108856.

[22] T. Xu et al., "High-gain integrated in-line few-mode amplifier enabling 3840-km long-haul transmission," *Photon. Res.*, vol. 10, no. 12, pp. 2794–2801, 2022.

[23] S. Jeurink and P. M. Krummrich, "Multimode EDFA with scalable mode selective gain control at 1480-nm pump wavelength," *IEEE Photon. Technol. Lett.*, vol. 30, no. 9, pp. 849–852, May 2018.

[24] C. Brunet, B. Ung, P.-A. Bélanger, Y. Messaddeq, S. LaRochelle, and L. A. Rusch, "Vector mode analysis of ring-core fibers: Design tools for spatial division multiplexing," *J. Lightw. Technol.*, vol. 32, no. 23, pp. 4648–4659, Dec. 2014.

[25] Y. Jung et al., "Three mode Er^{3+} ring-doped fiber amplifier for mode-division multiplexed transmission," *Opt. Exp.*, vol. 21, no. 8, pp. 10383–10392, 2013.

[26] R. Nasiri Mahalati, D. Askarov, and J. M. Kahn, "Adaptive modal gain equalization techniques in multi-mode erbium-doped fiber amplifiers," *J. Lightw. Technol.*, vol. 32, no. 11, pp. 2133–2143, Jun. 2014.

[27] J. H. Holland, "Genetic algorithms," *Sci. Amer.*, vol. 267, no. 1, pp. 66–73, 1992.

[28] S. Katoch et al., "A review on genetic algorithm: Past, present, and future," *Multimedia Tools Appl.*, vol. 80, pp. 8091–8126, 2021.

[29] H. Ding et al., "Multi-objective optimization of fiber laser cutting based on generalized regression neural network and non-dominated sorting genetic algorithm," *Infrared Phys. Technol.*, vol. 108, 2020, Art. no. 103337.

[30] A. Deng et al., "Analyzing mode index mismatch and field overlap for light guidance in negative-curvature fibers," *Opt. Exp.*, vol. 28, no. 19, pp. 27974–27988, 2020.

[31] M. Eguchi and Y. Tsuji, "Influence of reflected radiation waves caused by large mode field and large refractive index mismatches on splice loss evaluation between elliptical-hole lattice core holey fibers and conventional fibers," *JOSA B*, vol. 30, no. 2, pp. 410–420, 2013.

[32] M. Wada, T. Sakamoto, S. Aozasa, T. Mori, T. Yamamoto, and K. Nakajima, "Differential modal gain reduction of L-band 5-mode EDFA using EDF with center depressed core index," *J. Lightw. Technol.*, vol. 35, no. 4, pp. 762–767, Feb. 2017.

[33] F. Hakimian et al., "Optimization of a quantum-dot semiconductor optical amplifier (QD-SOA) design using the genetic algorithm," *Opt. Quantum Electron.*, vol. 52, no. 1, 2020, Art. no. 48.

[34] M. Z. Amin et al., "Doping radius effects on an erbium-doped fiber amplifier," *Chin. Opt. Lett.*, vol. 17, no. 1, 2019, Art. no. 010602.

[35] I. Amiri et al., "Pump laser automatic signal control for erbium-doped fiber amplifier gain, noise figure, and output spectral power," *J. Opt. Commun.*, 2019, doi: 10.1515/joc-2019-0203.

[36] D. M. Baney et al., "Theory and measurement techniques for the noise figure of optical amplifiers," *Opt. Fiber Technol.*, vol. 6, no. 2, pp. 122–154, 2000.

[37] A. M. Velázquez-Benítez et al., "Scaling photonic lanterns for space-division multiplexing," *Sci. Rep.*, vol. 8, no. 1, 2018, Art. no. 8897.

[38] S. N. Khonina et al., "Optical multiplexing techniques and their marriage for on-chip and optical fiber communication: A review," *Opto-Electron. Adv.*, vol. 5, no. 8, 2022, Art. no. 210127.

[39] J. J. Wu et al., "Advances in energy-level systems of organic lasers," *Laser Photon. Rev.*, vol. 16, no. 12, 2022, Art. no. 2200366.

[40] J. Shi et al., "Exciton character and high-performance stimulated emission of hybrid lead bromide perovskite polycrystalline film," *Adv. Opt. Mater.*, vol. 8, no. 10, 2020, Art. no. 1902026.